Agriculture, Ecosystems and Environment 292 (2020) 106821

Contents lists available at ScienceDirect

Agriculture, Ecosystems and Environment

journal homepage: www.elsevier.com/locate/agee

Characteristics of carbon, water, and energy fluxes on abandoned farmland revealed by critical zone observation in the karst region of southwest China

Yanwei Wang[a,b], Weijun Luo[a,c,*], Guangneng Zeng[d], Haijun Peng[a], Anyun Cheng[a,c], Lin Zhang[a,c], Xianli Cai[a,b,c], Jia Chen[a,b,c], Yina Lyu[a,b], Hanling Yang[a,b], Shijie Wang[a,c]

[a] State Key Laboratory of Environmental Geochemistry, Institute of Geochemistry, Chinese Academy of Sciences, Guiyang, 550081, China
[b] University of Chinese Academy of Sciences, Beijing, 100049, China
[c] Puding Karst Ecosystem Research Station, Chinese Academy of Sciences, Puding, 562100, China
[d] School of Chemistry and Eco-Environmental Engineering, Guizhou Minzu University, Guiyang, 550025, China

ARTICLE INFO

Keywords:
Karst critical zone
Abandoned farmland
Nature restoration
Carbon flux
Water flux

ABSTRACT

Extensive areas of agricultural land have been abandoned to ecological restoration in recent years in the karst region of Southwest China, which contributes to the greening of the area. However, there has yet no direct observation of carbon, water, and energy fluxes on abandoned land in the region. In addition, because of the coupling between above and below-ground processes, monitoring of the karst ecosystem needs to be conducted from a critical zone perspective. In this study, an integrated vertical observation system through air-vegetation-soil-cave continuums was constructed on abandoned farmland under natural restoration in Puding Karst Ecosystem Research Station. Preliminary results show that: First, vegetation cover restored rapidly after abandonment, and the measured net ecosystem exchange (NEE), soil CO_2 efflux, actual evapotranspiration (ET_a) and latent heat (LE) in the rainy season are about twice of that in the dry season, this strong seasonal variation relates to the typical subtropical monsoon climate with synchronous water and heat availability during rainy season. Second, high CO_2 concentrations and significant CO_2 variation in the monitored cave indicate that the exchange of underground carbon pools with the atmosphere cannot be neglected in the carbon budget of the study site.

1. Introduction

Agricultural expansion and intensification have caused land degradation, loss of biodiversity, and reduction of ecosystem service worldwide (Barral et al., 2015). In the karst region of Southwest China, because of its fragile nature and intensive land use, serious land degradation in the form of karst rocky desertification at a rate of 25,000 $km^2\ yr^{-1}$ once prevailed in the area (Cao et al., 2015; Jiang et al., 2014; Wang et al., 2004). With the transition of china's environmental management (He et al., 2012), a number of ecological projects have been implemented since the late 1990s to overcome the ecological degradation, such as the Natural Forest Protection Project, the Grain to Green Program (Sloping Land Conversion Program), and the Karst Rocky Desertification Comprehensive Control and Restoration Project (Qi et al., 2013; Tong et al., 2017; Xu et al., 2006). As a result, satellite time series data shows a widespread increase in leaf area index and aboveground biomass in the karst regions of southwest China (Brandt et al., 2018; Tong et al., 2018). Also, the subtropical forest in the East Asian monsoon region has one of the highest carbon uptakes of forests worldwide, and the primary reason may be the young stand ages and high nitrogen deposition, coupled with sufficient and synchronous water and heat availability (Yu et al., 2014). So the conversion of cropland to forest could significantly enhance carbon sequestration in Southwest China (Wang et al., 2017b). But to our knowledge, there has yet no direct observation of carbon uptake capacity on abandoned farmland at the early stage of natural restoration in the region.

Also, carbon cycle in karst ecosystem is complex compared to other terrestrial ecosystems, rough topography, discontinuous soil distribution, developed underground space, dissoluble carbonate rock, and adaptable plants led to a great challenge in quantifying carbon balance at ecosystem scale (Jiang et al., 2013; Song et al., 2017; Wang et al., 2017a). For example, FLUXNET is a global network of hundreds of micrometeorological flux measurements sites that measure the exchanges of carbon dioxide, water vapor, and energy between the biosphere and atmosphere greatly advanced our understanding of various terrestrial ecosystem in terms of ecosystem photosynthesis, ecosystem respiration and NEE (Baldocchi, 2008; Baldocchi et al., 2001; Oliphant, 2012), but the eddy covariance data of net CO_2 fluxes over karstic

* Corresponding author at: State Key Laboratory of Environmental Geochemistry, Institute of Geochemistry, Chinese Academy of Sciences, Guiyang, 550081, China.
E-mail address: luoweijun@vip.gyig.ac.cn (W. Luo).

https://doi.org/10.1016/j.agee.2020.106821
Received 2 July 2019; Received in revised form 14 December 2019; Accepted 9 January 2020
Available online 24 January 2020
0167-8809/

substrates sometimes was unusual in a biological context (Barraquer-Bordas et al., 2010; Kowalski et al., 2008; López-Ballesteros et al., 2017; Sanchez-Cañete et al., 2011). CO_2 dynamics within the karst ecosystem may be controlled by a number of processes that traditionally been neglected. Studies show that abiotic processes such as weathering and subterranean cave ventilation could contribute to the carbon budget on short times scales. For example, carbonate mineral weathering coupled with aquatic photosynthesis alone in the world karst region represents about 30 % of the terrestrial carbon sink (Liu et al., 2010, 2018). The underground space is fully developed in the karst region and the subterranean CO_2 concentration is much higher than the atmospheric background, which forms the secondary carbon pool (Benavente et al., 2010). This pool becomes a source of atmospheric CO_2 during the process of ventilation (Benavente et al., 2015; James et al., 2015; Lang et al., 2017). Essentially, the sources of this carbon pool come from the downward diffusion of soil respiration and the decay of infiltrated organic matter inside the vadose zone (Baldini et al., 2006; Sanchez-Moral et al., 2010). A first approximation estimates that the subterranean CO_2 pool and its potential ventilation could represent more than half of the total annual atmospheric sink (Serrano-Ortiz et al., 2010).

While *in situ* research and measurements have revealed much about the various physical, biological and chemical processes in each part of the karst ecosystem, there is a lack of tools to directly observe the functions of the karst ecosystem in a systematic approach. Here, based on the theory of critical zone science (Anderson et al., 2008; Covington, 2016; Guo and Lin, 2016; White et al., 2015), an observation system coupled with aboveground and belowground processes concurrently, using eddy covariance, automatic gas flux chamber and CO_2 profile to quantify interactions in the atmosphere-plant-soil-cave continuums was built. This integrated monitor platform is aimed at the long term and continues *in situ* observation of carbon, water, and energy fluxes on abandoned farmland at the early stage of natural restoration. To our knowledge, no comparable studies have been conducted before in the region. Our aims are: Firstly, investigate the magnitude and the seasonal characteristics and dynamics of carbon, water, and energy fluxes at the early stage of natural restoration. Secondly, investigate the interactions of carbon flux between the atmosphere and plant-soil-cave continuums from a vertical scale, namely from the perspective of the critical zone.

2. Materials and methods

2.1. Site description

The study site (26.36 °N, 105.76 °E, 1170 m.a.s.l) is located in Puding Karst Ecosystem Research Station in Puding County, Guizhou Province, Southwest China (Fig. 1). The region experiences a typical subtropical monsoon climate, with a mean annual temperature of 15.1℃ and a mean annual precipitation of 1,367 mm (Liu et al., 2016b). The dominant geology in the area is the limestone of the Guanling Formation of the Middle Triassic (Zeng et al., 2016). The abandoned farmland (More than *ca.* 50 years cultivation of corn and rapeseed) under natural restoration was established in 2010 and vegetation recovered rapidly since (Fig. 2). The vegetation is mainly tree-shrub-grass mosaic. Trees occupy approximately 22 % (mainly Pear, Plum, Hackberry, Aspen, Chinese toon and Catalpa), shrub occupies approximately 44 % (mainly Rubus coreanus, Pyracantha, Coriaria sinica maxim and Broussoneti ppeyrifer), and grass occupies approximately 8 % (mainly Cogon), respectively. The canopy height is uneven, with a single tree height ranges from 4 to 10 m, with shrub ranges from 1 to 2 m and grass less than 1 m. The soil type is limestone soil (Rendzina, in FAO soil taxonomy classifications) according to Chinese soil general classification. Soil depth is very uneven ranging from 0 m (rocky outcrops) to several meters in soil pockets between rocks. The percentage of soil organic matter in the topsoil (0 − 20 cm) is about 2.8 %, the total nitrogen is about 3.2 g kg^{-1}. The topography is rolling, which shows a relative altitude difference within 10 m. The rocky outcrop is approximately 40 % of the ground surface. There is a natural cave located in the center of the study site (Fig. 2). The accessible passage of the cave is about 10 m deep and 30 m long, and the cave entrance above the cave passage is 0.5 m^2 (Wang et al., 2019).

2.2. Measurement system

Critical zone refers to the zone from the upper vegetative canopy through groundwater which acts as a distinct co-evolving entity driven by physical, chemical, and biological processes (Brantley et al., 2017). Here, the karst critical zone includes boundary layer atmosphere, above-ground vegetation, surface soil, subsurface cave, and limestone bedrock (Fig. 3a). Carbon, water, and energy exchanges through each part of the karst critical zone. We select three key interfaces to study the characteristics of carbon exchange in the karst critical zone, includes the canopy-atmosphere interface, the soil-atmosphere interface, and the cave-atmosphere interface. Turbulent, diffusion and advection are the main exchange mechanisms between canopy and atmosphere, soil and atmosphere, cave and atmosphere, respectively (Fig. 3b).

For the first interface, the eddy covariance technique was used and a flux tower was installed at the southwest corner of the field (Fig. 2) considering the main wind direction is northeast. An open-path eddy covariance system consists of an open path infrared gas (CO_2 and H_2O) analyzer (IRGA) (LI-7500A, Li-Cor, Lincoln, NE, USA) and a sonic anemometer (Gill Windmaster Pro, Gill) was installed at 12.6 m on the flux tower. The LI-7500A was pointed toward the north at an angle of 20° to minimize solar radiation influence and to facilitate the shedding of water droplets from sensor lenses after rain events. Data from the sonic anemometer and the open path infrared gas analyzer were recorded at a frequency of 10 Hz using a data logger (LI-7550, Li-Cor, Lincoln, NE, USA). For the second interface, we used the LI-8100A Automated Soil CO_2 Flux System (Li-Cor, Lincoln, NE, USA) with eight long-term monitoring chambers (8100-104). Eight PVC soil collars (inner diameter 20.3 cm) were installed on the soil surface permanently and soil CO_2 efflux was measured every two-hours continuously. Small living plants in the soil collars were removed by hand regularly. Soil temperature (8150-203 probe) and soil moisture (Theta Probe ML2x) near chambers were also recorded at a depth of 5 cm of topsoil simultaneously. For the third interface, we used CO_2 Carbon Isotope Analyzer (CCIA-912-0003, LGR) to monitor CO_2 concentrations at different locations half-hourly throughout the cave system, including gas inlets inside cave passage, at cave entrance, at below 1 m and above 1 m of cave entrance, atmosphere air at 4 m, and soil air above the cave roof. Additionally, meteorological parameters were measured from a standard weather station (AMS) 100 m away from the flux tower (Fig. 2).

2.3. Data process and quality control

Turbulent fluxes of CO_2, H_2O, and energy between ecosystem and atmosphere were computed every half-hourly with the Eddypro software (6.1.0) (Biosciences, 2017; Fratini and Mauder, 2014). Main processing options including statistical analysis to screen spikes, insufficient amplitude resolution, drop-outs, values exceed absolute limits, skewness and kurtosis, discontinuities, time lags, angle of attack, and steadiness of horizontal wind (Vickers and Mahrt, 1997), block averaging, double-axis rotation for tilt correction, spectral correction, density fluctuations compensation, and quality check (Foken et al., 2004). Fluxes in Flag 2 and the out-of-range values were discarded. Gap filling and UStar-filtering were applied to the rest flux data using an online procedure that was recommended by FLUXNET and used as a standard by EUROFLUX and maintained by the Max Planck Institute (Papale et al., 2006; Reichstein et al., 2005; Wutzler et al., 2018). Daily and yearly sums of NEE, ET_a, LE, and H were calculated using gap-filled

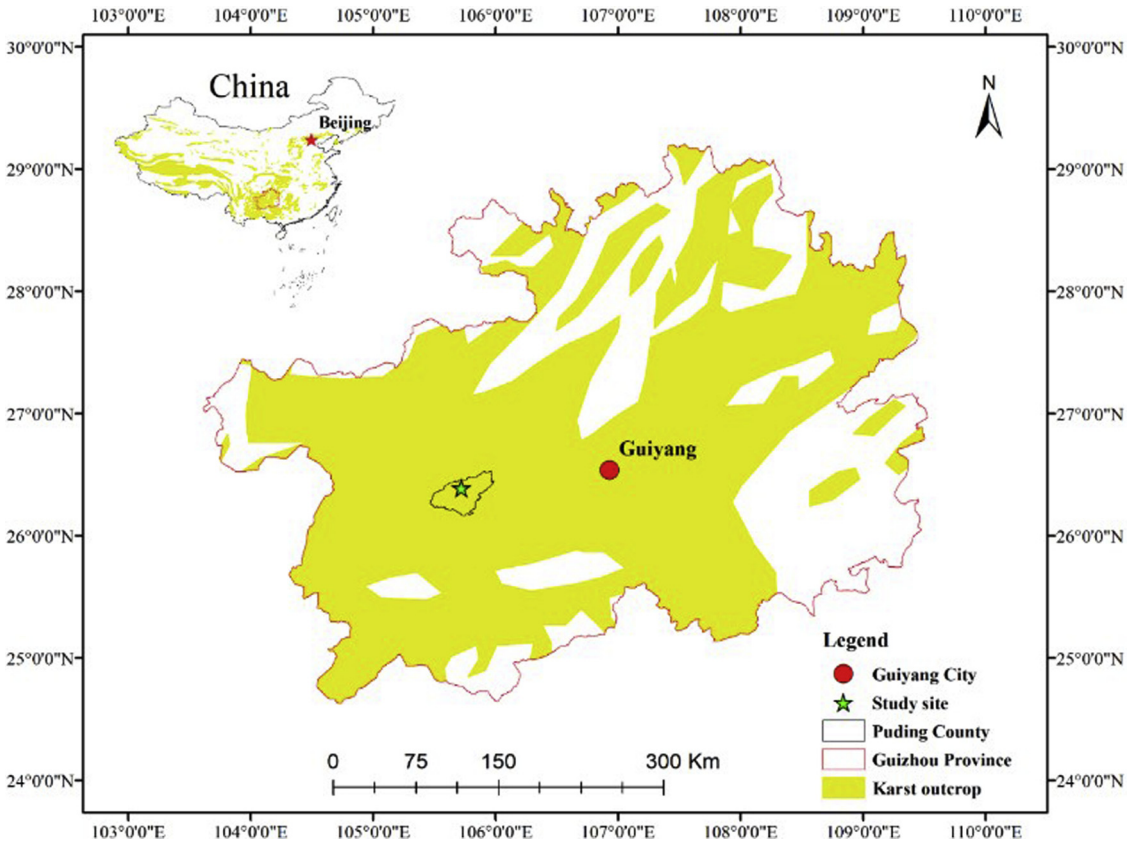

Fig. 1. Location of the study site.

data, where negative values indicate the net exchange from the atmosphere to the underneath ecosystem.

The soil CO_2 efflux was calculated using formulas as expressed below (Peng et al., 2015):

$$Fc = \frac{10VP_0(1 - W_0/1000)}{RS(T_0 + 273.15)}\frac{\partial C'}{\partial t}$$

Where Fc is soil CO_2 efflux (μmol m^{-2} s^{-1}). V is volume. P_0 is initial pressure. W_0 is initial water vapor mole fraction. S is soil surface area. T_0 is initial air temperature. R is gas constant. $\partial C'/\partial t$ is water-corrected initial chamber CO_2 mole fraction change rate. The initial change rate

Fig. 2. Views of land cover change and equipment distribution in the study site.

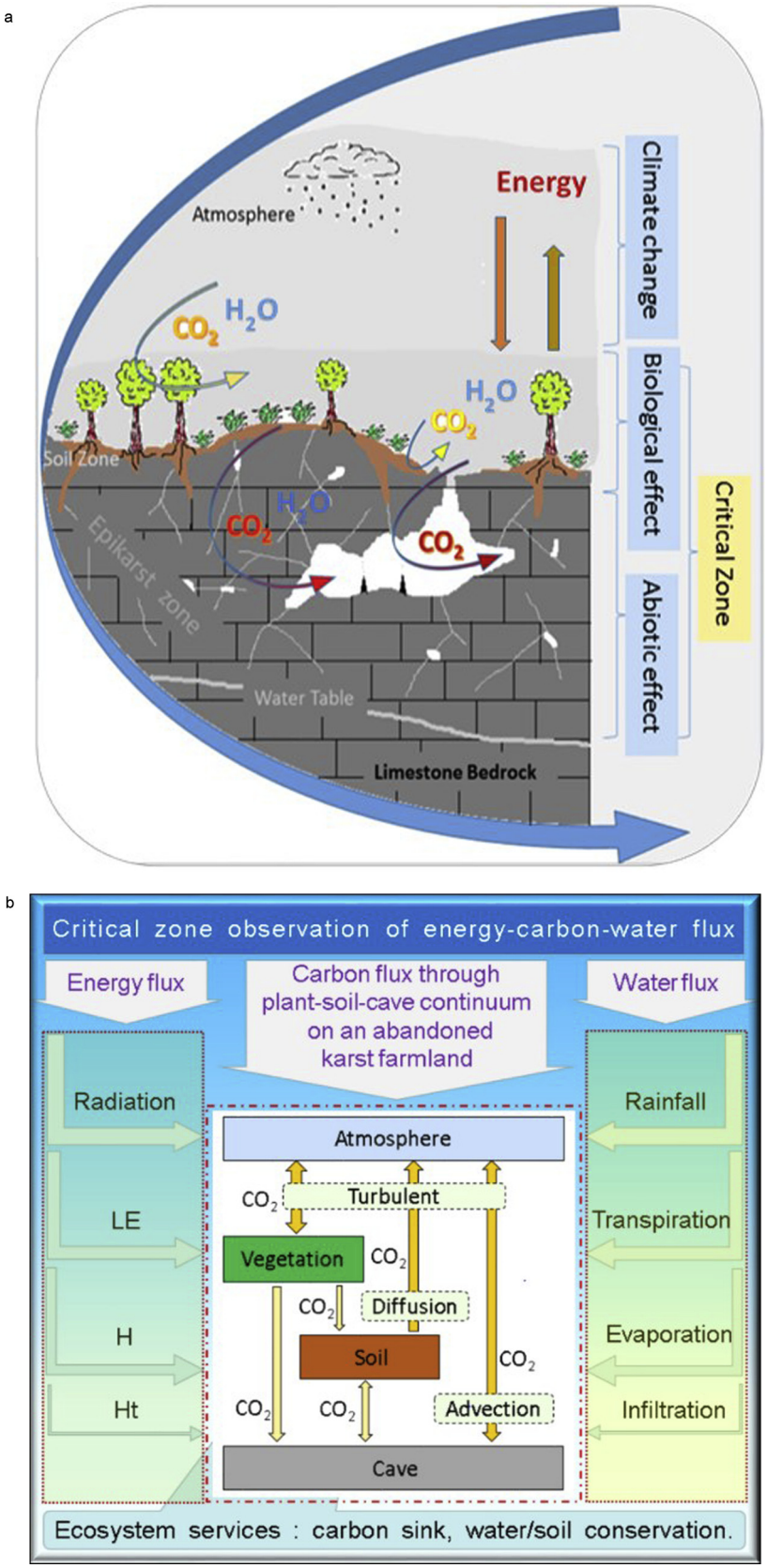

Fig. 3. a Schematic profile of karst critical zone. b Design of the integrated observation system.

was derived from exponential regression of CO_2 concentration change inside chamber. Only the results with a coefficient of determination larger than 0.99 were used. The missing data was gap filled with exponential model (Raich and Potter, 1995). Because of the spatial variability of chamber measurements, we choose the one which gave the median result to better represent the average soil CO_2 efflux level in

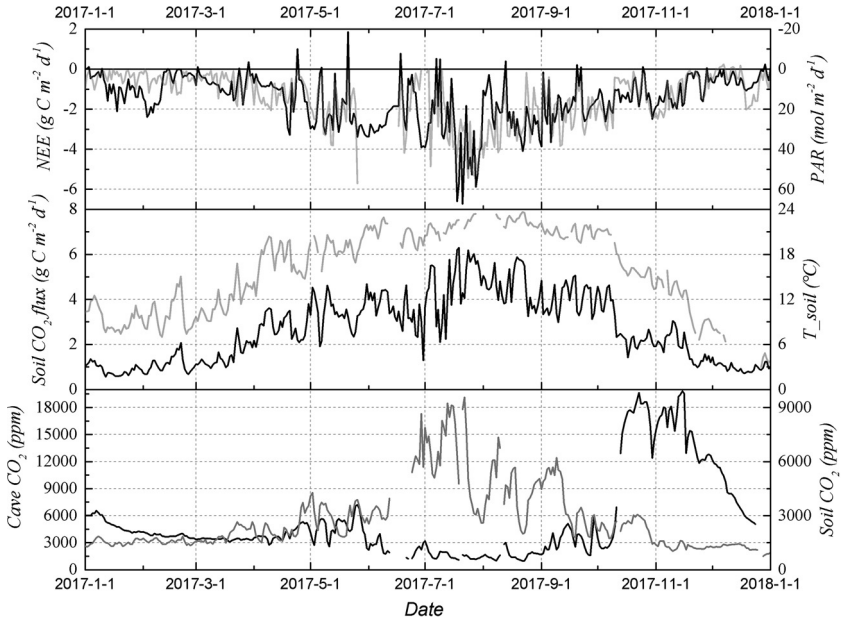

Fig. 4. Daily NEE, soil CO_2 flux, soil CO_2, cave CO_2, PAR, and soil temperature changes.
Black lines refer to parameters on the left axis and gray lines refer to parameters on the right axis.

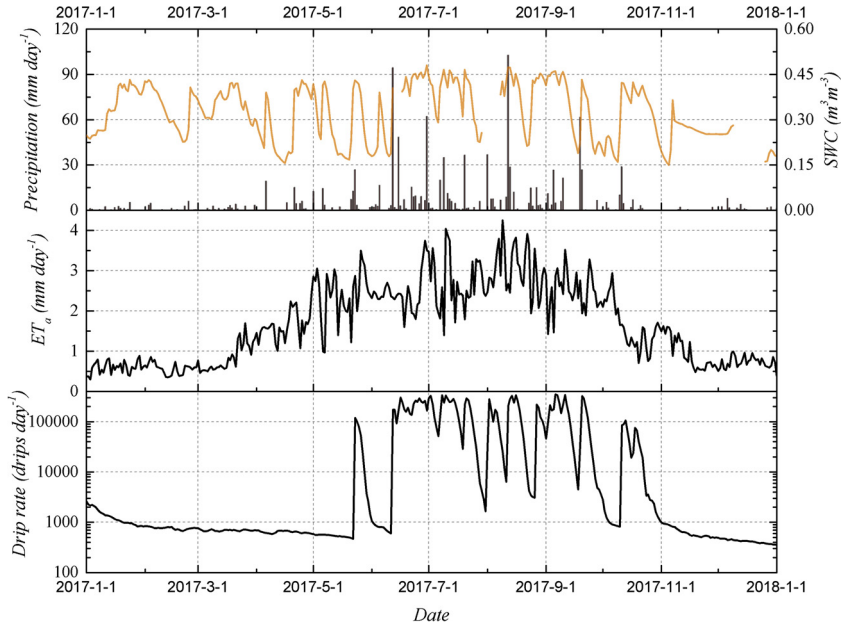

Fig. 5. Daily precipitation, SWC, ET_a, and drip rate changes.
Black lines refer to the parameters on the left axis and brown line refers to SWC.

this study.

The CO_2 Carbon Isotope Analyzer (CCIA-912-0003, LGR) measures CO_2 concentration from 380 ppm to 25,000 ppm at 1 HZ. It measures 120 s for each gas inlet cyclically and only the last 90 s were averaged as the final result. The analyzer was internal calibrated using one commercial reference gas (CO_2: 395 ppm, Ar: 1.01 %, O_2:21.6 %, the rest is N_2) weekly. The accuracy of CO_2 concentration measured was checked before and after each calibration using three reference gases (CO_2 concentration of 395 ppm, 7002 ppm, and 13,985 ppm). Because the relative errors were always within 1 %, so no external calibration was applied.

3. Results

3.1. CO_2 fluxes and concentration pattern through karst critical zone

For the observation period of 2017, the measured daily NEE changed seasonally and was generally negative which indicates overall net uptake of atmospheric CO_2 by the underlying ecosystem (Fig. 4). Average daily NEE was -1.5 g C m^{-2} d^{-1} and the annual sum was -559 g C m^{-2} with 73 % contributed from rainy season (May to October). The measured daily soil CO_2 efflux changed seasonally and was always positive which indicated net emission of CO_2 by soil surface (Fig. 4). The average daily soil CO_2 efflux was 2.7 g C m^{-2} d^{-1} and the annual sum was 979 g C m^{-2} d^{-1} with 72 % contributed from rainy season. Variations of daily NEE and soil CO_2 efflux generally followed

the pattern of photosynthetically active radiation (PAR) and soil temperature changes, respectively (Fig. 4). Soil temperature alone can explain 90 % of soil CO_2 efflux variability through exponential function while PAR can only explain 44 % of NEE variability through linear function. Annual PAR was 5441 mol m^{-2} with 74 % contributed from rainy season. Annual average daily soil temperature was 15.6 ℃, while during rainy season the average daily soil temperature was 20.3 ℃. Both soil and cave CO_2 concentrations were orders of magnitude higher than atmospheric background and showed substantial seasonal fluctuation (Fig. 4). Soil CO_2 changed between 873 to 9573 ppm while cave CO_2 changed between 972 to 19,814 ppm. Peak cave CO_2 lagged soil CO_2 by approx. 3 months (Fig. 4).

3.2. Water flux through karst critical zone

For the observation period of 2017, the annual precipitation was 1166 mm and 87 % was from rainy season (Fig. 5). The measured actual evapotranspiration (ET_a) changed seasonally and the annual sum was 610 mm with 74 % from rainy season (Fig. 5). The calculated annual potential evapotranspiration (ET_0) was 739 mm and rainy season alone occupies 67 % (Gao et al., 2016). Annual ET_a was 52 % of precipitation and 83 % of ET_0, while during rainy season were 44 % and 91 %, respectively. Overall, ET_a was less than ET_0 and ET_0 was far less than precipitation. This apparent contradiction may be caused by drought because of the fast infiltration and thin nature of karst soil, which can be evidenced by soil water content (SWC) and drip rate changes (Fig. 5). Daily average SWC showed fluctuation between 0.15 and 0.48 $m^3\ m^{-3}$ frequently (Fig. 6). Drip rate on the cave floor changed with precipitation occurrence and the magnitude during rainy season was two orders of magnitude higher than during dry season (Fig. 5).

3.3. Energy flux through karst critical zone

For the observation period of 2017, the daily net radiation (Rn) showed periodic variations and was positive in most situations (Fig. 6). The annual sum of daily Rn was 2016 MJ m^{-2} with 72 % from rainy season. The daily latent heat flux (LE) showed seasonal variations and was always positive (Fig. 6). The annual sum of daily LE was 1465 MJ m^{-2} with 74 % from rainy season. The daily sensible heat flux (H) showed less seasonal variations and was positive in most situations (Fig. 6). The annual sum of daily H was 655 MJ m^{-2} with 58 % from rainy season. The daily soil heat flux (Ht) showed opposite seasonal changes (Fig. 6). The annual sum of daily Ht was 101 MJ m^{-2} with 145 % from rainy season. Annual LE was more than twice of H which indicated that LE was the main part of energy consumption. The ratio between available energy (Rn-Ht) and estimated energy (LE + H) was about 1.1 which indicated an overall energy balance considering uncertainty caused by different measurement footprint representativeness.

4. Discussion

Ensuring grain security and mitigating climate change are priority in China. Study shows that if all cropland on slopes above 25° under high erosion is converted to forest or grassland, grain production will only decrease by 0.91 %, and this will not damage grain security in China (Lu et al., 2013). On the other hand, the converted areas from croplands to forests under the program could make a considerable contribution to China's carbon sink (Liu et al., 2014; Lu et al., 2018). Expanding croplands always comes at the cost of reduced carbon stocks in natural vegetation and soils (West et al., 2010). On the contrary, cropland abandonment and the following restoration can enhance various ecosystem services, including carbon stock capacity. During a succession, carbon accumulates as living woody biomass, as soil organic matter (SOC) or both. Field survey by "space for time" approach in Maolan karst ecosystem shows that vegetation especially the component of woody plants has the greatest influence on ecosystem carbon stocks during the recovery progress of karst forests, and the maximum carbon sequestration rate of Maolan karst forest ecosystems during natural restoration process is about 234 g C $m^{-2}\ a^{-1}$, and vegetation biomass carbon accumulation contributes 82 % of the total ecosystem carbon sequestration rate (Huang et al., 2015) (Fig. 7). Aboveground vegetation carbon increase in the early stage of succession mainly results from high recruitment of woody plants, while carbon accumulations in the later forests were mainly due to tree growth (Liu et al., 2016a). Study in Mediterranean region shows that invasion of woody plant species after abandonment of marginal agricultural land could significantly change carbon balance, and shifting annual NEE form source to an evident sink (Ferlan et al., 2011). Another study shows that

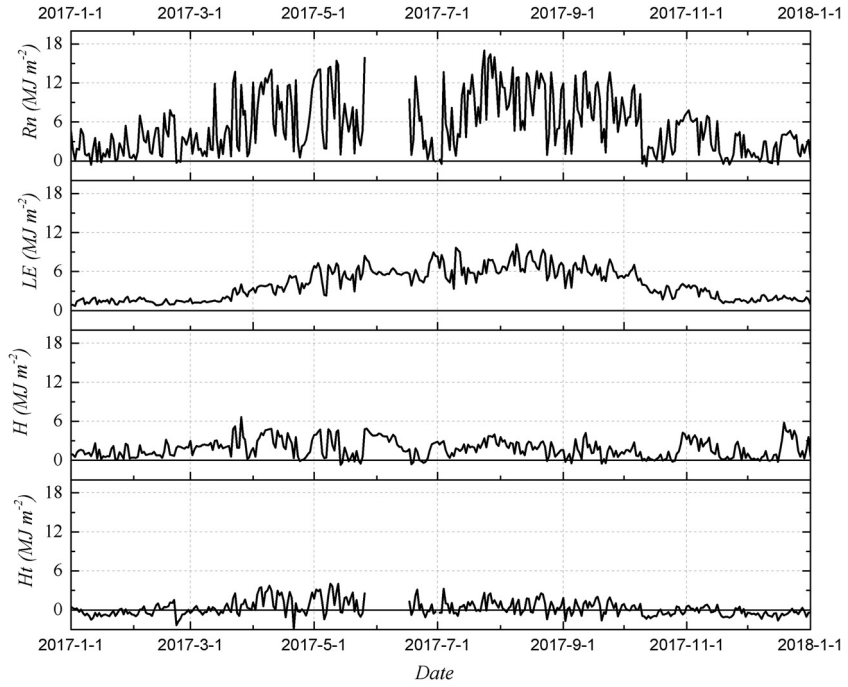

Fig. 6. Daily net radiation (Rn), latent heat (LE), sensible heat (H), and soil heat flux (Ht) changes.

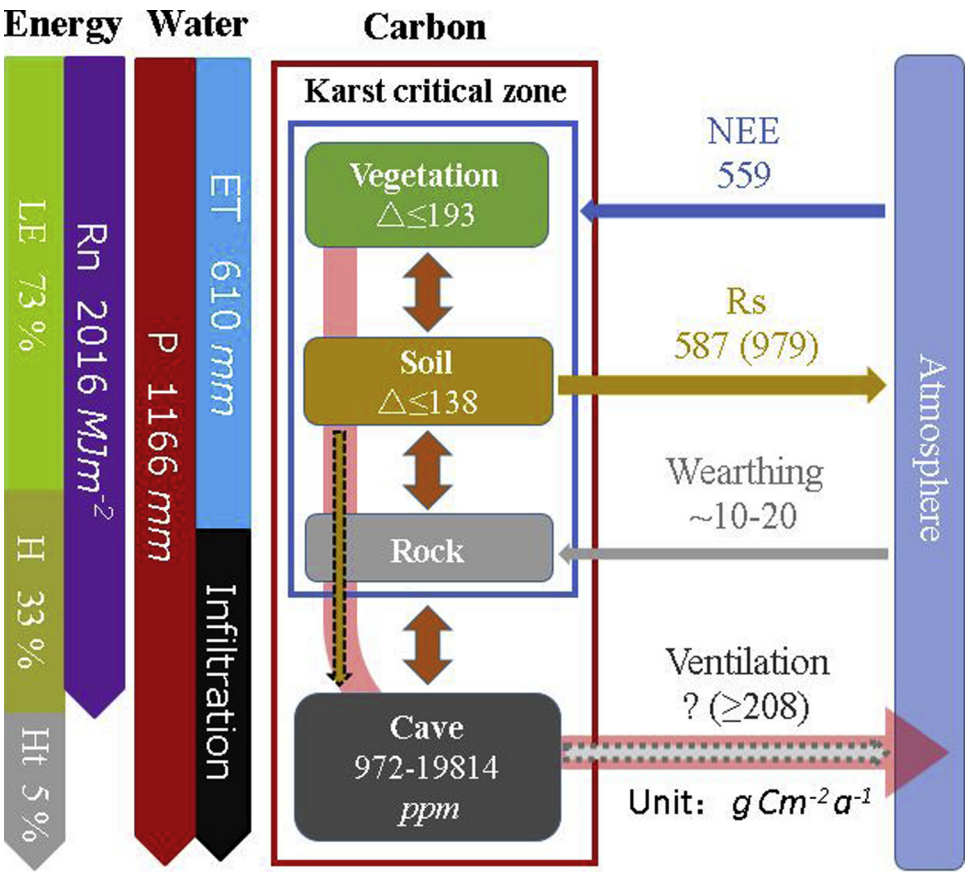

Fig. 7. The budget of carbon, water, and energy fluxes through karst critical zone during the 2017 period.
Δ refers change of carbon pool during succession. Rs in bracket is the measured soil CO_2 flux at the measurement point, while Rs outside the bracket is the soil CO_2 flux per unit area considered rock outcrop in the field. Ventilation magnitude in bracket is calculated from the difference between measured NEE and referenced potential changes of vegetation and soil carbon pool and carbon sink capacity related to carbonate weathering.

the agricultural abandonment and the following succession in the karst region are likely accompanied by rapid SOC accumulation with an average rate of 138 g C m^{-2} a^{-1} (Yang et al., 2016) (Fig. 7). And the rapidly recovered soil macro-aggregates after agricultural abandonment control the recuperation of SOC storage because most SOC is sequestrated by macro-aggregates (Liu et al., 2020).

The significant seasonal variability of carbon, water, and energy fluxes captured by flux tower measurement could be related to typical subtropical monsoon climate with synchronous water and heat availability during rainy season. And this seasonal variation pattern was different from similar studies in a Mediterranean climate (Ferlan et al., 2011, 2016). Although it is very difficult to judge the validity of eddy covariance measurements in open-canopy ecosystems by testing the energy budget closure for the possible large uncertainties in the estimation of the available energy (Anthoni et al., 1999). Acceptable agreement between energy fluxes measured by flux tower and available energy which is in the typical range for micrometeorological measurements is encouraging (Fig. 7). Combined with approximating ET_0 using ET_a, indicated that the results from flux tower measurements were reliable. However, the result of measured NEE is relatively too high to be explained by biological common sense alone. The average net ecosystem productivity of east Asian monsoon subtropical forests is 361 ± 39 g C m^{-2} a^{-1} (Yu et al., 2014), and the maximum potential carbon fluxes based on climate geographical statistical assessment is 554 g C m^{-2} a^{-1} for the study area (Zhu et al., 2014). For the monitored ecosystem is at its' seventh year of restoration, so its' NEE should not be higher (Besnard et al., 2018). Except for potential above-ground biomass increase and SOC change, we put forward the hypothesis that the overestimated NEE may be related to the below-ground carbonate weathering process and ventilation process of underground space. The carbon sink related to carbonate weathering is normally between 10–20 g C m^{-2} a^{-1} (Yan et al., 2011; Zeng et al., 2017) which is too small to account for the overestimated NEE (Fig. 7). So the ventilation process may be the main reason, force the ecosystem to carbon balance, and we get the magnitude of ventilation exchange should be at least 208 g C m^{-2} a^{-1} (Fig. 7), which is at the same order of magnitude as soil CO_2 efflux. Although subterranean space such as porosity, fractures, caves, and conduits usually occupy a small fraction of the rock volume, the fact that their hydraulic conductivity is much higher than that of surrounding rock gives them a crucial role in determining the flow direction, which is true to airflow too, combined with two orders of magnitude high of CO_2 concentration, makes sub-ground space an unique temporary pool and passage for mass flow (Fig. 7). For example, for a temperate pasture overlying an accessible cave, afternoon CO_2 emissions in summer are likewise inexplicable in a biological context, and rapid decreases of underground CO_2 molar fractions correlate well with sizeable CO_2 release to the atmosphere and should be accounted for in surface CO_2 exchange estimates (Kowalski et al., 2008; Sanchez-Cañete et al., 2011). In semi-arid Mediterranean ecosystems, a significant fraction of respired CO_2 is stored in the vadose zone and emitted afterward by subsoil ventilation, with subsoil ventilation contribution 0–23 % of the measured annual NEE (Serrano-Ortiz et al., 2014).

In conclusion, except efflux to the atmosphere through the soil surface, part of soil respired CO_2 can diffuse downward to underground spaces such as caves and fissures to form a temporary pool and become a point source to atmosphere later, the eddy covariance system cannot fully capture this part of ecosystem respiration because of the limited footprint, which will leads to the overestimated NEE in our study (Fig. 7). Similarly, the flux observation based on chamber measurements will underestimate the soil respiration in karst areas. In addition, great attention should be paid to the spatial discontinuity of soil distribution to avoid the overestimation of regional soil carbon emission (Fig. 7). These characteristics reflect the complexity and uniqueness of carbon cycle process in karst ecosystem. Because of the heterogeneity nature of karst ecosystem, a network of critical zone observatories is

needed to fully understand carbon cycle processes in karst landscape and to evaluate the contribution of underground secondary carbon pool to local and global carbon balance.

5. Conclusions

Our results demonstrate how *in situ* comprehensive observations from the perspective of critical zone can provide a full display of carbon, water, and energy exchange characteristics in the karst ecosystem. Although eddy covariance method itself has been successfully applied in complex underlying surfaces, attention should be paid according to local conditions when interpreting the results. Especially, the influence of underground ventilation process cannot be ignored in karst ecosystem. Abiotic processes together with biological processes contribute to the annual Net Ecosystem Carbon Balance. Natural restoration after farmland abandoned can contribute to mitigation aims by recovery of aboveground vegetation and soil carbon pool as well as enhancement of belowground process. The functions of karst critical zone under coupled climate and land cover change need long-term continuous observation.

Declaration of Competing Interest

The authors declare that they have no known competing financial interests or personal relationships that could have appeared to influence the work reported in this paper.

Acknowledgments

This work was supported by the National Key Research and Development Program of China [2016YFC0502300, 2016YFC0502102]; the Strategic Priority Research Program of Chinese Academy of Sciences [XDB40020100] the National Natural Science Foundation of China [41673121, 41663015, 41571130042 and 41571130074]; Foundation of Guizhou educational committeeKY [2016]159. We thank anonymous reviewers for their valuable comments and suggestions on this manuscript.

References

Anderson, S.P., Bales, R.C., Duffy, C.J., 2008. Critical Zone Observatories: building a network to advance interdisciplinary study of Earth surface processes. Mineral. Mag. 72 (1), 7–10.

Anthoni, P.M., Law, B.E., Unsworth, M.H., 1999. Carbon and water vapor exchange of an open-canopied ponderosa pine ecosystem. Agric. For. Meteorol. 95 (3), 151–168.

Baldini, J.U., Baldini, L.M., McDermott, F., Clipson, N., 2006. Carbon dioxide sources, sinks, and spatial variability in shallow temperate zone caves: evidence from Ballynamintra Cave, Ireland. J. Cave Karst Stud. 68 (1), 4–11.

Baldocchi, D., 2008. Breathing of the terrestrial biosphere: lessons learned from a global network of carbon dioxide flux measurement systems. Aust. J. Bot. 56 (1), 1–26.

Baldocchi, D., Falge, E., Gu, L.H., Olson, R., Hollinger, D., Running, S., et al., 2001. FLUXNET: a new tool to study the temporal and spatial variability of ecosystem-scale carbon dioxide, water vapor, and energy flux densities. Bull. Am. Meteorol. Soc. 82 (11), 2415–2434.

Barral, M.P., Benayas, J.M.R., Meli, P., Maceira, N.O., 2015. Quantifying the impacts of ecological restoration on biodiversity and ecosystem services in agroecosystems: a global meta-analysis. Agric. Ecosyst. Environ. 202, 223–231.

Barraquer-Bordas, L., Tolosa, E., Grau-Veciana, J.M., Salisachs-Rowe, P., 2010. Ventilation of subterranean CO_2 and Eddy covariance incongruities over carbonate ecosystems. Biogeosciences 7 (3), 859–867.

Benavente, J., Vadillo, I., Carrasco, F., Soler, A., Liñán, C., Moral, F., 2010. Air carbon dioxide contents in the vadose zone of a Mediterranean karst. Vadose Zone J. 9 (1), 126–136.

Benavente, J., Vadillo, I., Liñán, C., del Rosal, Y., Carrasco, F., 2015. Influence of the ventilation of a karst show cave on the surrounding vadose CO_2 reservoir (Nerja, South Spain). Environ. Earth Sci. 74 (12), 7731–7740.

Besnard, S., Carvalhais, N., Arain, M.A., Black, A., De Bruin, S., Buchmann, N., Cescatti, A., Chen, J.Q., Clevers, J.G.P.W., Desai, A.R., Gough, C.M., Havrankova, K., Herold, M., Hörtnagl, L., Jung, M., Knohl, A., Kruijt, B., Krupkova, L., Law, B.E., Lindroth, A., Noormets, A., Roupsard, O., Steinbrecher, R., Varlagin, A., Vincke, C., Reichstein, M., 2018. Quantifying the effect of forest age in annual net forest carbon balance. Environ. Res. Lett. 13 (12), 124018.

Biosciences, L., 2017. EddyPro Software Instruction Manual. LI-COR Inc., Lincoln, Nebraska, USA.

Brandt, M., Yue, Y.M., Wigneron, J.P., Tong, X.W., Tian, F., Jepsen, M.R., Xiao, X.M., Verger, A., Mialon, A., Al-Yaari, A., Wang, K.L., Fensholt, R., 2018. Satellite-observed major greening and biomass increase in South China Karst during recent decade. Earths Future 6 (7), 1017–1028.

Brantley, S.L., McDowell, W.H., Dietrich, W.E., White, T.S., Kumar, P., Anderson, S.P., Chorover, J., Lohse, K.A., Bales, R.C., Richter, D.D., Grant, G., Gaillardet, J., 2017. Designing a network of critical zone observatories to explore the living skin of the terrestrial Earth. Earth Surf. Dyn. 5 (4), 841–860.

Cao, J.H., Yuan, D.X., Tong, L.Q., Mallik, A., Yang, H., Huang, F., 2015. An overview of karst ecosystem in Southwest China: current state and future management. J. Resour. Ecol. 6 (4), 247–256.

Covington, M.D., 2016. 8. The importance of advection for CO_2 dynamics in the karst critical zone: an approach from dimensional analysis. Geological Society of America 516, 113–127.

Ferlan, M., Alberti, G., Eler, K., Batič, F., Peressotti, A., Miglietta, F., Zaldei, A., Simončič, P., Vodnik, D., 2011. Comparing carbon fluxes between different stages of secondary succession of a karst grassland. Agric. Ecosyst. Environ. 140 (1–2), 199–207.

Ferlan, M., Eler, K., Simončič, P., Batič, F., Vodnik, D., 2016. Carbon and water flux patterns of a drought-prone mid-succession ecosystem developed on abandoned karst grassland. Agric. Ecosyst. Environ. 220, 152–163.

Foken, T., Göockede, M., Mauder, M., Mahrt, L., Amiro, B., Munger, W., 2004. Post-field Data Quality Control, Handbook of Micrometeorology. Springer, pp. 181–208.

Fratini, G., Mauder, M., 2014. Towards a consistent eddy-covariance processing: an intercomparison of EddyPro and TK3. Atmos. Meas. Tech. 7 (7), 2273–2281.

Gao, X.L., Peng, S.Z., Wang, W.G., Xu, J.Z., Yang, S.H., 2016. Spatial and temporal distribution characteristics of reference evapotranspiration trends in Karst area: a case study in Guizhou Province, China. Meteorol. Atmos. Phys. 128 (5), 677–688.

Guo, L., Lin, H., 2016. Critical zone research and observatories: current status and future perspectives. Vadose Zone J. 15 (9).

He, G.Z., Lu, Y.L., Mol, A.P.J., Beckers, T., 2012. Changes and challenges: china's environmental management in transition. Environ. Dev. 3, 25–38.

Huang, Z.S., Yu, L.F., Fu, T.H., Yang, R., 2015. Characteristics of carbon sequestration during natural restoration of Maolan karst forest ecosystems. Chinese J. Plant Ecol. 39 (6), 554–564 (in Chinese with English Abstract).

James, E.W., Banner, J.L., Hardt, B., 2015. A global model for cave ventilation and seasonal bias in speleothem paleoclimate records. Geochem. Geophys. Geosystems 16 (4), 1044–1051.

Jiang, Z.C., Lian, Y.Q., Qin, X.Q., 2013. Carbon cycle in the epikarst systems and its ecological effects in South China. Environ. Earth Sci. 68 (1), 151–158.

Jiang, Z.C., Lian, Y.Q., Qin, X.Q., 2014. Rocky desertification in Southwest China: impacts, causes, and restoration. Earth. Rev. 132, 1–12.

Kowalski, A.S., Serrano-Ortiz, P., Janssens, I.A., Sánchez-Moral, S., Cuezva, S., Domingo, F., Were, A., Alados-Arboledas, L., 2008. Can flux tower research neglect geochemical CO_2 exchange? Agric. For. Meteorol. 148 (6–7), 1045–1054.

Lang, M., Faimon, J., Godissart, J., Ek, C., 2017. Carbon dioxide seasonality in dynamically ventilated caves: the role of advective fluxes. Theor. Appl. Climatol. 1–18.

Liu, C.C., Liu, Y.G., Guo, K., Wang, S.J., Liu, H.M., Zhao, H.W., Qiao, X.G., Hou, D.J., Li, S.B., 2016a. Aboveground carbon stock, allocation and sequestration potential during vegetation recovery in the karst region of southwestern China: a case study at a watershed scale. Agric. Ecosyst. Environ. 235, 91–100.

Liu, D., Chen, Y., Cai, W.W., Dong, W.J., Xiao, J.F., Chen, J.Q., Zhang, H.C., Xia, J.Z., Yuan, W.P., 2014. The contribution of China's Grain to Green Program to carbon sequestration. Landsc. Ecol. 29 (10), 1675–1688.

Liu, L.B., Wu, Y.Y., Zhang, Z.H., Cheng, A.Y., Ni, J., 2016b. Biomass of karst evergreen and deciduous broad-leaved mixed forest in central Guizhou province, southwestern China: a comprehensive inventory of a 2 ha plot. Silva Fenn. 50 (3), 1492.

Liu, M., Han, G.L., Zhang, Q., 2020. Effects of agricultural abandonment on soil aggregation, soil organic carbon storage and stabilization: results from observation in a small karst catchment, Southwest China. Agric. Ecosyst. Environ. 288.

Liu, Z.H., Dreybrodt, W., Wang, H.J., 2010. A new direction in effective accounting for the atmospheric CO_2 budget: considering the combined action of carbonate dissolution, the global water cycle and photosynthetic uptake of DIC by aquatic organisms. Earth. Rev. 99 (3–4), 162–172.

Liu, Z.H., Macpherson, G.L., Groves, C., Martin, J.B., Yuan, D.X., Zeng, S.B., 2018. Large and active CO_2 uptake by coupled carbonate weathering. Earth. Rev. 182, 42–49.

López-Ballesteros, A., Serrano-Ortiz, P., Kowalski, A.S., Sánchez-Cañete, E.P., Scott, R.L., Domingo, F., 2017. Subterranean ventilation of allochthonous CO_2 governs net CO_2 exchange in a semiarid Mediterranean grassland. Agric. For. Meteorol. 234–235, 115–126.

Lu, F., Hu, H.F., Sun, W.J., Zhu, J.J., Liu, G.B., Zhou, W.M., et al., 2018. Effects of national ecological restoration projects on carbon sequestration in China from 2001 to 2010. Proc. Natl. Acad. Sci. U. S. A. 115 (16), 4039–4044.

Lu, Q.S., Xu, B., Liang, F.Y., Gao, Z.Q., Ning, J.C., 2013. Influences of the Grain-for-Green project on grain security in southern China. Ecol. Indic. 34, 616–622.

Oliphant, A.J., 2012. Terrestrial ecosystem-atmosphere exchange of CO_2, water and energy from FLUXNET; Review and meta-analysis of a global in-situ observatory. Geogr. Compass 6 (12), 689–705.

Papale, D., Reichstein, M., Aubinet, M., Canfora, E., Bernhofer, C., Kutsch, W., Longdoz, B., Rambal, S., Valentini, R., Vesala, T., 2006. Towards a standardized processing of net ecosystem exchange measured with eddy covariance technique: algorithms and uncertainty estimation. Biogeosciences 3 (4), 571–583.

Peng, H.J., Hong, B., Hong, Y.T., Zhu, Y.X., Cai, C., Yuan, L.G., Wng, Y., 2015. Annual ecosystem respiration variability of alpine peatland on the eastern Qinghai-Tibet Plateau and its controlling factors. Environ. Monit. Assess. 187 (9), 550.

Qi, X.K., Wang, K.L., Zhang, C.H., 2013. Effectiveness of ecological restoration projects in

a karst region of southwest China assessed using vegetation succession mapping. Ecol. Eng. 54, 245–253.
Raich, J.W., Potter, C.S., 1995. Global patterns of carbon dioxide emissions from soils. Global Biogeochem. Cycles 9 (1), 23–36.
Reichstein, M., Falge, E., Baldocchi, D., Papale, D., Aubinet, M., Berbigier, P., Bernhofer, C., Buchmann, N., Gilmanov, T., Granier, A., Grunwald, T., Havrankova, K., Ilvesniemi, H., Janous, D., Knohl, A., Laurila, T., Lohila, A., Loustau, D., Matteucci, G., Meyers, T., Miglietta, F., Ourcival, J.M., Pumpanen, J., Rambal, S., Rotenberg, E., Sanz, M., Tenhunen, J., Seufert, G., Vaccari, F., Vesala, T., Yakir, D., Valentini, R., 2005. On the separation of net ecosystem exchange into assimilation and ecosystem respiration: review and improved algorithm. Glob. Chang. Biol. 11 (9), 1424–1439.
Sanchez-Cañete, E.P., Serrano-Ortiz, P., Kowalski, A.S., Oyonarte, C., Domingo, F., 2011. Subterranean CO_2 ventilation and its role in the net ecosystem carbon balance of a karstic shrubland. Geophys. Res. Lett. 38 (9), 159–164.
Sanchez-Moral, S., Cuezva, S., Fernández-Cortés, A., Benavente, D., Cañaveras, J., 2010. Effect of Ventilation on Karst System Equilibrium (Altamira Cave, N Spain): an Appraisal of Karst Contribution to the Global Carbon Cycle Balance, Advances in Research in Karst Media. Springer, pp. 469–474.
Serrano-Ortiz, P., Oyonarte, C., Pérez-Priego, O., Reverter, B.R., Sánchez-Cañete, E.P., Were, A., Uclés, O., Morillas, L., Domingo, F., 2014. Ecological functioning in grass-shrub Mediterranean ecosystems measured by eddy covariance. Oecologia 175 (3), 1005–1017.
Serrano-Ortiz, P., Roland, M., Sanchez-Moral, S., Janssens, I.A., Domingo, F., Goddéris, Y., Kowalski, A.S., 2010. Hidden, abiotic CO_2 flows and gaseous reservoirs in the terrestrial carbon cycle: review and perspectives. Agric. For. Meteorol. 150 (3), 321–329.
Song, X.W., Gao, Y., Wen, X.F., Guo, D.L., Yu, G.R., He, N.P., Zhang, J.Z., 2017. Carbon sequestration potential and its eco-service function in the karst area, China. J. Geogr. Sci. 27 (8), 967–980.
Tong, X.W., Brandt, M., Yue, Y.M., Horion, S., Wang, K.L., Keersmaecker, W.D., Tian, F., Schurgers, G., Xiao, X.M., Luo, Y.P., Chen, C., Myneni, R., Shi, Z., Chen, H.S., Fensholt, R., 2018. Increased vegetation growth and carbon stock in China karst via ecological engineering. Nat. Sustain. 1 (1), 44–50.
Tong, X.W., Wang, K.L., Yue, Y.M., Brandt, M., Liu, B., Zhang, C.H., Liao, C.J., Fensholt, R., 2017. Quantifying the effectiveness of ecological restoration projects on long-term vegetation dynamics in the karst regions of Southwest China. Int. J. Appl. Earth Obs. Geoinf. 54, 105–113.
Vickers, D., Mahrt, L., 1997. Quality control and flux sampling problems for tower and aircraft data. J. Atmos. Oceanic Technol. 14 (3), 512–526.
Wang, S.J., Liu, Z.H., Ni, J., Yan, J.H., Liu, X.M., 2017a. A review of research progress and future prospective of carbon cycle in karst area of South China. Earth & Environment 45 (1), 2–9 (in Chinese with English Abstract).
Wang, S.J., Liu, Q.M., Zhang, D.F., 2004. Karst rocky desertification in southwestern China: geomorphology, landuse, impact and rehabilitation. Land Degrad. Dev. 15 (2), 115–121.
Wang, X.G., Zhou, M.H., Li, T., Ke, Y., Zhu, B., 2017b. Land use change effects on ecosystem carbon budget in the Sichuan Basin of Southwest China: conversion of cropland to forest ecosystem. Sci. Total Environ. 609, 556–562.
Wang, Y.W., Luo, W.J., Zeng, G.N., Wang, Y., Yang, H.L., Wang, M.F., Zhang, L., Cai, X.L., Chen, J., Cheng, A.Y., Wang, S.J., 2019. High ^{222}Rn concentrations and dynamics in Shawan Cave, southwest China. J. Environ. Radioact. 199–200, 16–24.
West, P.C., Gibbs, H.K., Monfreda, C., Wagner, J., Barford, C.C., Carpenter, S.R., Foley, J.A., 2010. Trading carbon for food: global comparison of carbon stocks vs. Crop yields on agricultural land. Proc. Natl. Acad. Sci. U. S. A. 107 (46), 19645–19648.
White, T., Brantley, S., Banwart, S., Chorover, J., Dietrich, W., Derry, L., Lohse, K., Anderson, S., Aufdendkampe, A., Bales, R., Kumar, P., Richter, D., McDowell, B., 2015. The role of critical zone observatories in critical zone science. Develop. Earth Surf. Process. 15–78.
Wutzler, T., Lucas-Moffat, A., Migliavacca, M., Knauer, J., Sickel, K., Šigut, L., Menzer, O., Reichstein, M., 2018. Basic and extensible post-processing of eddy covariance flux data with REddyProc. Biogeosciences 15 (16), 5015–5030.
Xu, J.T., Yin, R.S., Li, Z., Liu, C., 2006. China's ecological rehabilitation: unprecedented efforts, dramatic impacts, and requisite policies. Ecol. Econ. 57 (4), 595–607.
Yan, J.H., Wang, Y.P., Zhou, G.Y., Li, S.G., Yu, G.R., Li, K., 2011. Carbon uptake by karsts in the Houzhai Basin, southwest China. J. Geophys. Res. 116 (G4).
Yang, L.Q., Luo, P., Wen, L., Li, D.J., 2016. Soil organic carbon accumulation during post-agricultural succession in a karst area, southwest China. Sci. Rep. Ist. Super. Sanita 6, 37118.
Yu, G.R., Chen, Z., Piao, S., Peng, C.H., Ciais, P., Wang, Q.F., Li, X.R., Zhu, X.J., 2014. High carbon dioxide uptake by subtropical forest ecosystems in the East Asian monsoon region. Proc. Natl. Acad. Sci. U. S. A. 111 (13), 4910–4915.
Zeng, C., Liu, Z.H., Zhao, M., Yang, R., 2016. Hydrologically-driven variations in the karst-related carbon sink fluxes: insights from high-resolution monitoring of three karst catchments in Southwest China. J. Hydrol. (Amst) 533, 74–90.
Zeng, Q.R., Liu, Z.H., Chen, B., Hu, Y.D., Zeng, S.B., Zeng, C., Yang, R., He, H.B., Zhu, H., Cai, X.L., Chen, J., Ou, Y., 2017. Carbonate weathering-related carbon sink fluxes under different land uses: a case study from the Shawan Simulation Test Site, Puding, Southwest China. Chem. Geol. 474, 58–71.
Zhu, X.J., Yu, G.R., He, H.L., Wang, Q.F., Chen, Z., Gao, Y.N., Zhang, Y.P., Zhang, H.J., Yan, J.H., Wang, H.M., Zhou, G.S., Jia, B.R., Xiang, W.H., Li, Y.N., Zhao, L., Wang, Y.F., Shi, P.L., Chen, S.P., Xin, X.P., Zhao, F.H., Wang, Y.L., Tong, C.L., Fu, Y.L., Wen, X.F., Liu, Y.C., Zhang, L.M., Zhang, L., Su, W., Li, S.G., Sun, X.M., 2014. Geographical statistical assessments of carbon fluxes in terrestrial ecosystems of China: results from upscaling network observations. Glob. Planet. Change 118, 52–61.